Estimation of Ionosphere-Compensated Azimuth Ground Motion with Sentinel-1

Giorgio Gomba, German Aerospace Center (DLR), Oberpfaffenhofen, Germany, email: giorgio.gomba@dlr.de

Abstract

This paper deals with the mitigation of ionospheric effects in the estimation of azimuth ground motion using Sentinel-1 images. Thanks to the high accuracy of Sentinel-1 azimuth orbit timings, precise absolute measurements of azimuth ground displacements are possible, nevertheless, variations in the ionosphere electron content can introduce significant errors. Azimuth shifts are usually estimated with the Enhanced Spectral Diversity technique in the burst overlap areas. The ionospheric phase contribution can be estimated with the split-spectrum method. In this paper, the correction of ionospheric errors in azimuth shifts is realized by compensating the ionospheric phase in the burst overlap areas; this is only possible when considering the correct ionospheric height and the squint angles. The technique is thoroughly described in the paper. Experiments shows how this procedure can sensibly mitigate the ionospheric influence on azimuth shifts, improving the measurements of geophysical phenomena as, for example, earthquakes.

1 Introduction

Ground movements that occur between two Sentinel-1 acquisitions are estimated by measuring the mutual shifts between the images. Spatial variations in the ionospheric electron density can change the azimuth position of objects in the image causing the ground motion measurement to be imprecise.

With Sentinel-1 TOPS mode data, the azimuth mutual shifts between images are usually measured in the burst overlap areas by applying the Enhanced Spectral Diversity (ESD) technique [1]. The high Doppler separation of the two bursts in the overlap area permits to obtain a higher accuracy with respect to the non-overlapping parts. However, due to the different squint angles of the two overlapping bursts, the radio waves travel through two different parts of the ionosphere. Therefore, if the ionosphere electron content at the two piercing points is different, the measured azimuth shift is biased. Only the compensation of the ionospheric phase in the piercing points reduces the azimuth shift error. An estimation of the ionospheric phase, as well as height, is thus necessary. The split-spectrum method can estimate the differential relative ionospheric phase screen [2, 3]. Therefore, it is possible to compensate the ionospheric phase in the burst overlaps to obtain correct ground movement measurements. The accuracy of the compensation depends on the estimation accuracy of the split-spectrum method. The ionospheric height is iteratively estimated by minimization of the residual ESD azimuth shifts. The complete correction procedure is thoroughly described in Section 2. Section 3 presents a Sentinel-1 example which contains a strong ionospheric variation. The compensated interferogram and azimuth shifts are also presented.

2 Technique

With respect to the implementation of the split-spectrum method for burst mode data that has been presented in [3], the processing has been simplified and improved. A significant difference with the procedure illustrated in [2] and [3] is that only the unwrapping of the fullband scene interferogram is now required. This reduces the processing complexity, caused by the possibility of phase unwrapping errors, by eliminating the need of the differential phase unwrapping errors correction described in [2]. A detailed description of the whole process follows:

(I) *Standard Sentinel-1 Processing*

Firstly, a standard Sentinel-1 processing as in [4] is performed. A global azimuth offset is estimated with ESD, the bursts are resampled, mosaicked, and a scene interferogram is generated. The fullband scene interferogram is then unwrapped. Possible indicators of high ionospheric activity are: a) phase ramps in the interferograms; b) a high azimuth offset, which is due to the linear part of the azimuth ionospheric variation; c) a high variation of the offsets at the single burst overlaps, usually present with phase jumps at burst intersections, which are due to the nonlinear part of the ionospheric variation.

(II) *Subbands Generation*

The split spectrum method requires that two range subbands of one third of the total spectrum are produced [2], this can be realized by band-pass filtering the bursts. After filtering, the subbands must be demodulated to baseband to avoid phase biases during the resampling. After demodulation, the two subbands are resampled separately. Both subband-filtering and resampling are applied on each single burst separately. Alternatively, one can band-pass filter the resampled fullband bursts, however, the frequency dependent phase which is added by the resampling shift must then be removed.

(III) *Interferograms Generation*

The DEM-based simulated phase is scaled to the subband carrier frequencies and used to produce two subband interferograms for each burst with same multilooking as in the fullband one.

(IV) *Ionospheric Phase Estimation*

The following step calculates the raw ionospheric phase.

The interferometric phases of the lower and higher subbands, respectively $\Delta\phi_L$ and $\Delta\phi_H$, can be written as:

$$\begin{aligned}\Delta\phi_L &= \Delta\phi_{non\text{-}disp}\frac{f_L}{f_0} + \Delta\phi_{iono}\frac{f_0}{f_L} + 2\pi N,\\ \Delta\phi_H &= \Delta\phi_{non\text{-}disp}\frac{f_H}{f_0} + \Delta\phi_{iono}\frac{f_0}{f_H} + 2\pi M,\end{aligned} \quad (1)$$

where $\Delta\phi_{non\text{-}disp}$ is the non dispersive phase, $\Delta\phi_{iono}$ is the ionospheric phase, f_0 is the fullband carrier frequency, f_L and f_H are respectively the carrier frequency of the lower and upper subbands, and M and N represent unknown phase cycles. The Delta-k phase [5] is:

$$\begin{aligned}\phi_{\Delta k} &= \angle[\exp(j(\Delta\phi_L - \Delta\phi_H))]\\ &= \Delta\phi_{non\text{-}disp}\frac{f_L - f_H}{f_0} + \Delta\phi_{iono}\left(\frac{f_0}{f_L} - \frac{f_0}{f_H}\right).\end{aligned} \quad (2)$$

Unwrapping is not necessary since an ionospheric variation within the burst of at least 300 TEC would be required to wrap this phase, which is unrealistic. The non-dispersive term is also unlikely to wrap the Delta-k phase, since it is multiplied by the small factor $\Delta f/f_0$, where Δf is the subbands separation. The unwrapped fullband phase is:

$$\Delta\phi = \Delta\phi_{non\text{-}disp} + \Delta\phi_{iono}. \quad (3)$$

Combining the (3) with the (2), we obtain the raw ionospheric phase:

$$\Delta\phi_{iono} = \left(\Delta\phi - \phi_{\Delta k}\frac{f_0}{f_L - f_H}\right)\frac{f_L f_H}{f_L f_H + f_0^2}. \quad (4)$$

(V) *Ionospheric Height Estimation*

The ionospheric height is found automatically with an iterative procedure. The ionospheric piercing points of each estimated pixel are calculated using the timing and the Doppler information for a fixed supposed ionospheric height. A robust low-order polynomial fitting is then applied to the noisy raw ionospheric phase to filter it, with the ionospheric phase pixels positioned at the calculated piercing points. The ESD phase is then recalculated at each burst overlap, with the addition of two correcting phase terms. Since the bursts have been resampled according to the first ESD estimation of the azimuth offset, the ESD phase will be close to zero (apart from deviations due to nonlinear ionospheric variations). Therefore, the first correcting term in this version of the ESD is the phase which is proportional to the removed offset:

$$\phi_{ESD} = 2\pi\Delta f_{DC}^{ovl}\frac{\Delta y}{f_{az}}, \quad (5)$$

where Δf_{DC}^{ovl} is the Doppler centroid frequency difference in the overlap area, Δy is the offset in pixels, and f_{az} is the image azimuth sampling frequency [4]. This brings the ESD phase back to the original phase prior to the resampling. The second correcting term is the ionospheric phase, calculated using the fitted polynomial parameters and projecting the overlap area at the ionospheric height in the two different positions for the two burst, according to the squint angles.

A robust linear fitting in the azimuth direction is then applied to the estimated ESD shifts, which should all yield zero if the chosen ionospheric height is correct and no ground motion is present. The linear fitting allows for a small deviation if an orbit error trend is present, when long stripes of continuous frames are processed. The robust algorithm ensures that eventual ground motion, as for example caused by an earthquake, is not taken into consideration for the linear fitting. This procedure is then repeated iteratively until the ionospheric height that minimizes the residual shifts is found, the parameters of the linear fitting are used as a cost for the minimization. The iterations find the ionospheric height that minimizes the offset and the linear trend of the residual shifts.

(V) *Ionospheric Phase Screen Generation*

After the best ionospheric height is found, the final smooth ionospheric phase screen can be produced. The noisy raw ionospheric estimates, projected at their positions defined by the ionospheric height, timing and squint angles, are fitted with a robust low-order polynomial. The fitting residuals are filtered to extract remaining undulations. The filter size is automatically adapted to remove the noise and maintain the ionospheric undulations with a variogram analysis that permits to establish the correct cutoff frequency of the filter. The filter window is a Matérn function [6], but a simpler Gaussian window can also be used.

The final scene interferogram is then produced compensating each single burst with the correct part of the ionospheric phase screen. The final azimuth shifts are estimated with the compensated ESD phase.

3 Experiment

An earthquake occurred occurred 46 km offshore from Illapel, Chile on September 16, 2015. Various Sentinel-1 acquisitions cover the area, it is then possible to form interferograms with different orbits and looking angles. Figure 1 shows one example, produced with four images acquired in an ascending orbit on September 2, 2015 and four acquired on October 20, 2015. Figure 2 shows the mutual azimuth shifts measured with ESD at the burst overlaps separated in smaller blocks, and filtered with a Gaussian window to fill the voids between the overlaps for visualization purposes. The original blocks in the burst overlaps are superimposed on the filtered shifts. Figure 3 shows, in blue, the average azimuth shift at each burst overlap for the three swaths.

Since the acquisitions are at low latitudes and in the afternoon, ionospheric disturbances are very probable as high levels of electron density in the equatorial regions are usually followed by strong gradients. In fact, the example interferogram presents many fringes which are due to the electron content variation in the ionosphere. For the same reason, the azimuth shifts have an offset of about 30 cm.

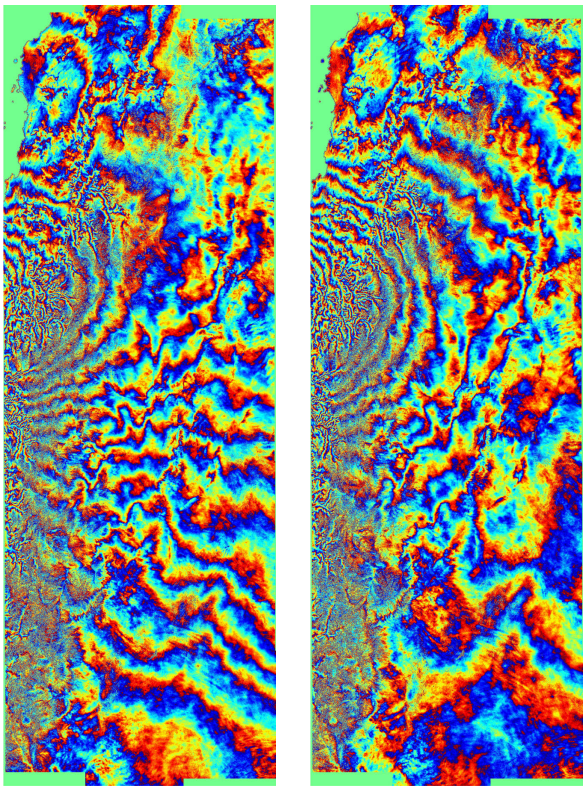

Figure 1: Original Sentinel-1 interferogram of the 2015 Illapel earthquake (left) and after ionosphere compensation (right).

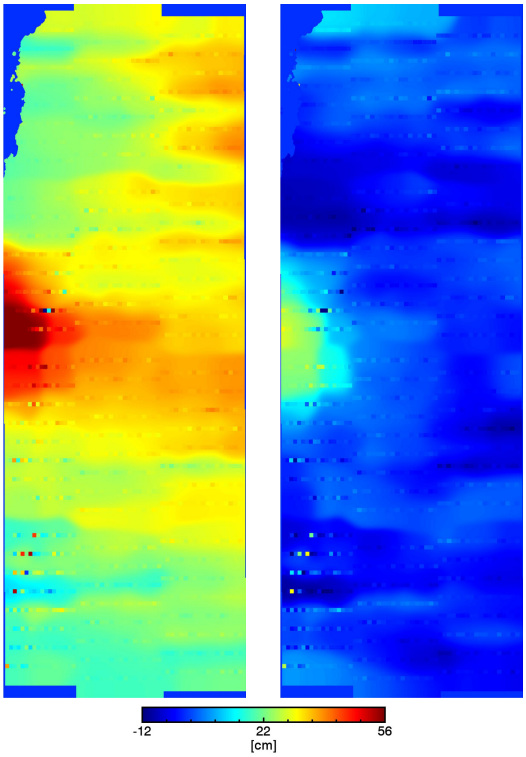

Figure 2: Original Sentinel-1 azimuth shifts of the 2015 Illapel earthquake (left) and after ionosphere compensation (right), measured with ESD at the burst overlaps separated in smaller blocks and filtered with a Gaussian window to fill the voids between the overlaps for visualization purposes. The ESD blocks in the burst overlaps are superimposed on the filtered shifts.

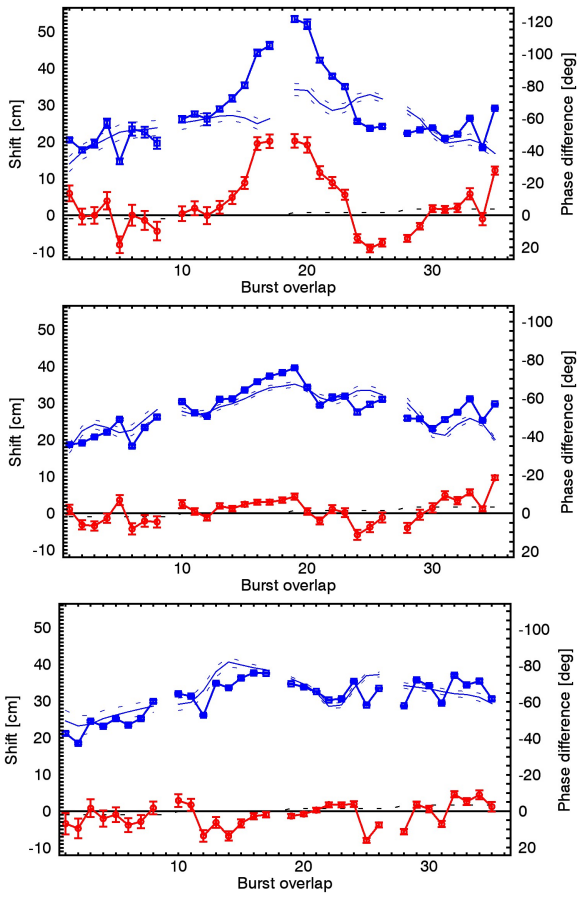

Figure 3: Azimuth shift, with error bars, measured at burst overlaps with ESD, before (blue), and after (red) ionospheric correction. The thin blue line is the estimated ionospheric shift with its accuracy (dashed line). Top: left swath, bottom: right swath.

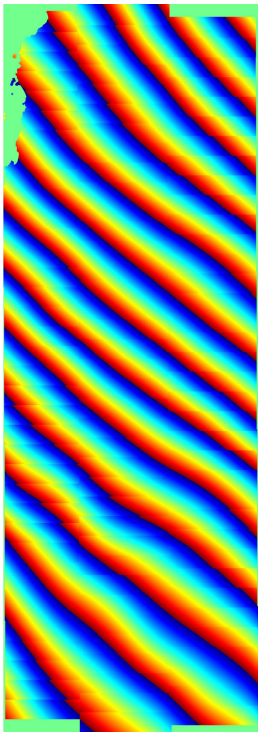

Figure 4: Ionospheric phase screen estimated with the split-spectrum method.

After applying the split spectrum method described in Section 2, the presence of an ionospheric variation in the azimuth direction which creates the undesired effects is confirmed. The estimated ionospheric phase screen is shown in Figure 4, the compensated interferogram in Figure 1, and the compensated azimuth shifts are in Figure 2 and 3.

4 Conclusions

Ionospheric variations can introduce errors in the estimation of along track ground motion. These effects have been shown to reach also several meters when using L-band images. With C-band data, we show in this paper that the azimuth ionospheric error can reach the half meter level. This can be a critical problem for various application, as for example, earthquakes modeling or fault parameters estimation. Furthermore, we show that it is possible to reduce such errors to a centimeter level, by applying the split-spectrum method and using its estimation of the ionosphere also to correct the ESD azimuth shift. Correction of cross-correlation azimuth shifts and their combination with ESD is also possible. This permits to fully exploit the high precision of the Sentinel-1 orbits and system. With respect to the common practice of removing trends from the estimated motion fields, the proposed technique might improve the estimation of geophysical parameters in earthquake or fault modeling.

References

[1] P. Prats-Iraola, R. Scheiber, L. Marotti, S. Wollstadt, and A. Reigber. TOPS Interferometry With TerraSAR-X. *IEEE Transactions on Geoscience and Remote Sensing*, 50(8):3179–3188, Aug 2012.

[2] G. Gomba, A. Parizzi, F. De Zan, M. Eineder, and R. Bamler. Toward Operational Compensation of Ionospheric Effects in SAR Interferograms: The Split-Spectrum Method. *IEEE Transactions on Geoscience and Remote Sensing*, 54(3):1446–1461, March 2016.

[3] G. Gomba, F. Rodríguez González, and F. De Zan. Ionospheric Phase Screen Compensation for the Sentinel-1 TOPS and ALOS-2 ScanSAR Modes. *IEEE Transactions on Geoscience and Remote Sensing*, 55(1):223–235, Jan 2017.

[4] N. Yagüe-Martínez, P. Prats-Iraola, F. Rodríguez González, R. Brcic, R. Shau, D. Geudtner, M. Eineder, and R. Bamler. Interferometric Processing of Sentinel-1 TOPS Data. *IEEE Transactions on Geoscience and Remote Sensing*, 54(4):2220–2234, April 2016.

[5] R. Bamler and M. Eineder. Accuracy of differential shift estimation by correlation and split-bandwidth interferometry for wideband and delta-k sar systems. *Geoscience and Remote Sensing Letters, IEEE*, 2(2):151–155, April 2005.

[6] G. Gomba and F. De Zan. Bayesian Data Combination for the Estimation of Ionospheric Effects in SAR Interferograms. *IEEE Transactions on Geoscience and Remote Sensing*, 55(11):6582–6593, Nov 2017.